1521-009X/43/12/1838–1846$25.00
Drug Metabolism and Disposition

http://dx.doi.org/10.1124/dmd.115.065482
Drug Metab Dispos 43:1838–1846, December 2015

Xenobiotic Metabolism in Mice Lacking the UDP-Glucuronosyltransferase 2 Family[S]

Matthew J. Fay, My Trang Nguyen, John N. Snouwaert, Rebecca Dye, Delores J. Grant, Wanda M. Bodnar, and Beverly H. Koller

Department of Genetics (M.J.F., M.T.N., J.N.S., R.D.), Department of Environmental Sciences and Engineering (W.M.B.), and Department of Medicine, Pulmonary and Critical Care Division (B.H.K.), University of North Carolina at Chapel Hill, Chapel Hill, North Carolina; and Department of Biology and Cancer Research Program, JLC-Biomedical/Biotechnology Research Institute, North Carolina Central University, Durham, North Carolina (D.J.G.)

Received June 8, 2015; accepted September 8, 2015

ABSTRACT

UDP-Glucuronosyltransferases (UGTs) conjugate a glucuronyl group from glucuronic acid to a wide range of lipophilic substrates to form a hydrophilic glucuronide conjugate. The glucuronide generally has decreased bioactivity and increased water solubility to facilitate excretion. Glucuronidation represents an important detoxification pathway for both endogenous waste products and xenobiotics, including drugs and harmful industrial chemicals. Two clinically significant families of UGT enzymes are present in mammals: UGT1s and UGT2s. Although the two families are distinct in gene structure, studies using recombinant enzymes have shown considerable overlap in their ability to glucuronidate many substrates, often obscuring the relative importance of the two families in the clearance of particular substrates in vivo. To address this limitation, we have generated a mouse line, termed *ΔUgt2*, in which the entire *Ugt2* gene family, extending over 609 kilobase pairs, is excised. This mouse line provides a means to determine the contributions of the two UGT families in vivo. We demonstrate the utility of these animals by defining for the first time the in vivo contributions of the UGT1 and UGT2 families to glucuronidation of the environmental estrogenic agent bisphenol A (BPA). The highest activity toward this chemical is reported for human and rodent UGT2 enzymes. Surprisingly, our studies using the *ΔUgt2* mice demonstrate that, while both UGT1 and UGT2 isoforms can conjugate BPA, clearance is largely dependent on UGT1s.

Introduction

UDP-Glucuronosyltransferases (UGTs) are membrane-bound phase II enzymes that conjugate a wide array of lipophilic substrates with a glucuronyl group from UDP-glucuronic acid (UDPGA). The highly polar glucuronide conjugate generally decreases the bioactivity of the substrate and increases its water solubility, facilitating excretion through bile or urine. Glucuronidation is important in the metabolism of endogenous wastes and a wide range of drugs, including many chemotherapeutics, nonsteroidal anti-inflammatory drugs, and opioids, and in protecting against harmful environmental agents such as bisphenol A (BPA) and benzo-[*a*]-pyrene (Fang et al., 2002; Hanioka et al., 2008; Kutsuno et al., 2013). Based on evolutionary divergence and homology, mammalian UGTs have been organized into two major families: The UGT1 and UGT2 families. The mammalian UGT1 family currently contains only the UGT1A subfamily, while the mammalian UGT2 family contains the UGT2A and UGT2B subfamilies (Mackenzie et al., 2005; Rowland et al., 2013).

This work was supported by the United States Public Health Service [Grants ES021838 and HL107780]; the National Institute of Environmental Health Sciences [Grant P30ES010126]; and SURF and Taylor Honors Research Fellowship grants from UNC-Chapel Hill.

dx.doi.org/10.1124/dmd.115.065482.

[S]This article has supplemental material available at dmd.aspetjournals.org.

The mouse UGT1 family is encoded by the *Ugt1a* gene. It consists of nine functional isoforms, each encoded by a unique 5′ exon spliced to a shared set of downstream exons (Mackenzie et al., 2005). The first exon specifies a UGT1A isoform and its substrate specificity, while the downstream exons encode common domains such as a UDPGA binding site and a transmembrane region (Owens et al., 2005). The three *Ugt2a* and seven *Ugt2b* genes in mouse are located in a single cluster spanning approximately 600 kilobase pairs (kbp) on chromosome 5 (Mackenzie et al., 2005). *Ugt2a1* and *Ugt2a2*, similar to *Ugt1a*, have unique first exons and a shared set of downstream exons (Jedlitschky et al., 1999). All other *Ugt2* genes have a typical structure, with unique exons encoding both the N-terminal substrate-binding domain and a C-terminal UDPGA-binding domain and transmembrane sequence (Hum et al., 1999). Similar to the UGT1 family, the C-terminal domains of the UGT2 family are conserved, while the highly variable N-terminal domains determine substrate specificity (Radominska-Pandya et al., 1999). Many UGT isoforms exhibit activity toward a broad range of substrates, and the specificities of different isoforms often overlap (de Wildt et al., 1999).

Various approaches have been used to determine which UGTs are involved in glucuronidation of particular compounds (Rowland et al., 2013). Assignment using computational approaches is limited by the lack of established structure-activity relations for most UGTs (Kaivosaari, 2010). The majority of current knowledge comes from assessment of metabolism of substrates by microsomes reconstituted with

ABBREVIATIONS: BPA, bisphenol A; BPAG, bisphenol A glucuronide; ES, embryonic stem; HPLC, high-performance liquid chromatography; kbp, kilobase pair; napG, naproxen glucuronide; PCR, polymerase chain reaction; UDPGA, UDP-glucuronic acid; UGT, UDP-glucuronosyltransferase; WT, wild type.

recombinant enzymes. Such studies have shown that UGT2s are involved in conjugation of a variety of endogenous metabolites, such as retinoic acid and steroid hormones, as well as xenobiotics, such as opioid analgesics (Hum et al., 1999; Radominska-Pandya et al., 2001; Chouinard et al., 2007). While information from these studies can be used to predict the relative importance of various enzymes in vivo, extrapolation of in vitro results to in vivo systems remains an imperfect practice (Lin and Wong, 2002; Miners et al., 2006). Such modeling has to take into account not only the activities of the enzymes toward the substrate under study but also the fact that there are quantitative and qualitative differences in the expression of these enzymes in the tissues exposed to the chemical. Ultimately, in vivo metabolism is required to confirm the contribution of particular UGT enzymes to the metabolism of a compound. However, due to the functional overlap of many isoforms, it is often difficult to measure the contributions of one isoform or even one UGT family in vivo.

These challenges have been encountered in defining the contributions of different UGTs to metabolism and clearance of environmental pollutants such as BPA, a monomer commonly used in polycarbonate materials with widespread human exposure. BPA's reported toxicity in mice at low doses (Richter et al., 2007), possibly through interference in both genomic and nongenomic estrogen responses (Luconi et al., 2002), has made it the subject of intense research (Krishnan et al., 1993). The ability of BPA to impact physiologic processes is likely limited by the rapid clearance of the inactive bisphenol A glucuronide (BPAG) (Matthews et al., 2001; Völkel et al., 2002), and studies with recombinant enzymes indicate that human UGT2B15 and rodent UGT2B1 likely play the primary role in clearance (Yokota et al., 1999; Hanioka et al., 2008). This has raised concerns regarding exposure of neonates to BPA (Ginsberg and Rice, 2009), since expression of UGT2 genes during the neonatal period is much lower than in children and adults (Coughtrie et al., 1988; de Wildt et al., 1999; Divakaran et al., 2014). Despite extensive efforts toward understanding the health impact of BPA exposure, remarkably little is known regarding its metabolic pathways in human or in the model organisms used in assessing its adverse effects.

To address these limitations, we have generated a mouse line homozygous for a targeted deletion of the entire *Ugt2* family. We show that loss of these enzymes does not adversely affect the development of these animals, and that microsomes from mice lacking all *Ugt2* genes can be used to establish the role of the UGT2 enzymes in glucuronidation of xenobiotics. Most importantly, this mouse line can be used to investigate the contribution of UGT2 enzymes to the metabolism of drugs and xenobiotics in vivo.

Materials and Methods

Reagents and Materials. Alamethicin and (S)-naproxen were purchased from Cayman Chemical (Ann Arbor, MI). BPA, BPAG, UDPGA, and β-glucuronidase were purchased from Sigma-Aldrich (St. Louis, MO). Naproxen glucuronide (napG) [(S)-naproxen acyl β-D glucuronide] was purchased from Toronto Research Chemicals (Toronto). All solvents and other reagents were of analytical grade or better. Zorbax Eclipse XDB-C18 and Tosoh TSKGel 80TM columns were purchased from Agilent Technologies (Santa Clara, CA) and Tosoh Bioscience (Tokyo), respectively. Primer sequences can be found in Supplemental Material.

Generation of Mouse Lines. A replacement-type targeting vector was assembled from 129 bacterial artificial chromosomes bMQ357m23 and bMQ37h06. DNA corresponding to the *Ugt2* gene cluster was replaced with a neomycin-resistance gene driven by the phosphoglycerate kinase promoter. Homologous recombination of the targeting vector with the endogenous *Ugt2* locus creates a 609 kbp deletion extending from 580 base pairs downstream from the *Ugt2b34* gene to 7.2 kbp upstream of the *Ugt2a1/2* gene. 129S6-derived embryonic stem (ES) cells were cultured using standard methods, and DNA was introduced by electroporation. Cells were selected in Geneticin and were evaluated by polymerase chain reaction (PCR) and Southern blot analysis. Correctly targeted ES cells were introduced into C56BL/6 blastocysts and the blastocysts introduced into B6D2F1/J foster mothers to complete their development. All mice were maintained in specific pathogen–free housing in ventilated caging. 129S6 mice purchased from Taconic (Hudson, NY) were bred to chimeras to maintain the deleted locus on this genetic background. All mice used in these studies are therefore 129S6, coisogenic for the deleted *Ugt2* locus. For all studies of reproductive function, wild-type (WT) and null mice were generated by the intercross of heterozygous animals. Serum testosterone levels were measured by enzyme-linked immunosorbent assay (Endocrine Technologies, Newark, CA). For some experiments mutant mice were age and sex matched at weaning and housed together until used in an experiment. All studies were conducted in accordance with the National institutes of Health *Guide for the Care and Use of Laboratory Animals* (National Research Council, 2011) as well as the Institutional Animal Care and Use Committee guidelines for the University of North Carolina at Chapel Hill.

Gene Expression Assays. Total RNA was isolated from tissue homogenates using a Quick-RNA Miniprep Kit (Zymo Research, Irvine, CA), and reverse transcription PCR was performed using a High Capacity cDNA Reverse Transcription Kit (Life Technologies, Grand Island, NY). cDNA was amplified with the FastStart Universal Probe Master with Rox normalization (Roche Applied Science, Indiana, IN), and *Ugt1* and *Ugt2* expressions were measured using SYBR Green quantitative PCR primers and TaqMan quantitative PCR probe mixes (Life Technologies), respectively. Amplifications were performed in duplicate on a QuantStudio 6 Flex Real-Time PCR System (Life Technologies). Data were analyzed using the comparative threshold cycle method as described by Applied Biosystems (Waltham, MA). Relative expression was determined by normalizing samples to 18S rRNA expression.

Microsome Preparation. Liver microsomes were prepared from 3 to 5 month old males. Median and left lobes of each liver were harvested after systemic perfusion with phosphate-buffered saline and homogenized manually in 0.05 M phosphate buffer (pH 7.4) with 0.154 M potassium chloride and 0.25 M sucrose. Homogenate was centrifuged twice at 10,000*g* for 10 minutes, and the postmitochondrial fraction was removed and centrifuged at 100,000*g* for 45 minutes. Microsomal pellets were washed with homogenization buffer and resuspended in 0.1 M phosphate buffer (pH 7.4) with 20% glycerol (v/v) and 1 mM EDTA. All preparation steps were performed at 4°C. Microsomal protein concentration was determined using Bio-Rad Protein Assay Dye (Bio-Rad Laboratories, Hercules, CA) with bovine serum albumin as a standard. Microsomes were stored at −80°C until used and underwent no more than one freeze/thaw cycle before experimentation.

High-Performance Liquid Chromatography (HPLC). HPLC was performed on an Agilent Technologies 1200 Series instrument. The system is comprised of a binary solvent pump with temperature-controlled autosampler, on-line degasser, variable-wavelength UV-visible detector, temperature-controlled column oven, and automated fraction collector. Chromatographic protocols are detailed in Table 1. Identities of all glucuronide peaks were verified by comparison with an authentic standard and by loss of the peak after β-glucuronidase treatment.

Microsomal Glucuronidation Assays. Glucuronidation reaction mixtures contained 0.1 M Tris buffer (pH 7.5), 4 mM magnesium chloride, substrate, and the indicated amount of microsomes in a final volume of 500 μl. Total organic solvent concentrations were less than 0.7% (v/v). Naproxen glucuronidation reactions contained 25 μg/ml alamethicin; BPA glucuronidation was performed both with and without alamethicin. After preincubation on ice and preheating at 37°C for 5 minutes, reactions were initiated by addition of UDPGA to a final concentration of 5 mM and incubated at 37°C. Reactions were terminated by addition to an equal volume of ice-cold 4% acetic acid in methanol (v/v) and vortex mixing. Microsomal protein was removed by centrifugation at 10,000*g* for 10 minutes at 4°C, and 30 μl of supernatant was analyzed by HPLC. Controls included baseline measurements and blanks lacking UDPGA. Glucuronide cleavage was performed by incubation of samples with 1000 units of β-glucuronidase for 4 hours at pH 5 to 6. Retention times for naproxen and its glurcuronide, napG, were 8.4 and 4.7 minutes, respectively. Consistent with previous studies (Bowalgaha et al., 2005), the napG standard was unstable, and napG was quantified based on a standard curve for naproxen, which was linear in

TABLE 1

Chromatographic protocols

The aqueous solvent (A) was 0.1% acetic acid in water (v/v) and the organic solvent (B) was 0.1% acetic acid in acetonitrile (v/v). The autosampler chamber was held at 6°C, and columns were held at 25°C for all experiments. The protocol for BPA in vivo is based on that of Yokota et al. (1999).

Assay	Column	λ	Flow Rate	Elution Program
		nm	*ml/min*	
Naproxen in vitro	Zorbax Eclipse XDB-C18 (150 × 4.6 mm, 5μm)	225	1.50	30% B from 0 to 5 minutes Linear increase to 70% B from 5 to 5.5 minutes Linear increase to70% B from 5.5 to 10 minutes
BPA in vitro	Zorbax Eclipse XDB-C18 (150 × 4.6 mm, 5μm)	280	0.50	15% B from 0 to 4.5 minutes Linear increase to 60% B from 4.5 to 5 minutes Linear increase to 60% B from 5 to 16 minutes
BPA in vivo	Tosoh TSKgel ODS 80TM (250 × 4.6 mm, 5 μm)	280	1.00	Isocratic 35% B

the range of 1–100 μM ($r^2 > 0.999$). The lower limit of detection was 1 μM for naproxen and napG. Retention times for BPA and BPAG were 15.2 and 12.8 minutes, respectively. Standard curves for BPA and BPAG were linear in the range of 0.5 μM to 1 mM ($r^2 > 0.999$ for both), and the lower limit of quantification was 0.5 μM for BPA and BPAG. Kinetics data were analyzed using Microsoft Excel 2010 and GraphPad Prism version 4.0 software (GraphPad Software, La Jolla, CA).

In Vivo BPA Glucuronidation. Age- and weight-matched WT and *ΔUgt2* mice were anesthetized with urethane, and the bile duct was cannulated. After collection of a sample of bile prior to dosage, mice received BPA intravenously as a bolus in 10% ethanol/water (v/v). Two BPA dosage levels were examined: 2 and 20 mg BPA/kg b.wt. Bile fractions were collected in 10 minute intervals over the next 50 minutes. Samples were diluted 1:40 in deionized water, and 30 μl of each sample were analyzed by HPLC. Retention time for BPAG was 5.7 minutes. Standard curves for BPAG were linear in the range of 0.5 μM to 1 mM ($r^2 > 0.999$) and the lower limit of quantification was 0.5 μM for BPA and BPAG.

Results

Generation of Mouse Line and Verification of *ΔUgt2* Locus. The *Ugt2* genes are located in a segment of DNA on chromosome 5 between *Ythdc1* and *Sult1b1* (Fig. 1). While numerous polymorphisms distinguish the *Ugt2* locus of the 129 strain from that of C57BL/6, no difference in the number and overall organization of the genes was identified by PCR, sequence, or Southern blot analysis. Therefore, using the organization of the published C57BL/6 locus as a guide, we generated a targeting vector designed to remove the entire gene family in a single recombination event in 129 derived ES cells. The deletion was designed to leave the *Ythdc1* and *Sult1b1* genes, including regulatory regions, intact (Fig. 1). *Sult1b1* encodes a sulfotransferase enzyme that contributes to conjugation and excretion of endo- and xenobiotics, and therefore any compromise in the expression of this gene would complicate interpretation of the phenotypes of the UGT2-deficient animals. ES cells were identified where the targeting vector had integrated into the *Ugt2* locus. These were analyzed to ensure that the recombination event had occurred at the predicted locations in the mouse genome and had resulted in loss of all *Ugt2* genes. This analysis included extensive PCR, sequence, and Southern blot analyses. ES cells that met these criteria were used to generate a mouse line. For simplicity, we refer to this mutation as the *ΔUgt2* allele. The *ΔUgt2* allele was maintained on the 129S6 genetic background by breeding transmitting chimeras to purchased 129S6 dams. Mice heterozygous for the deletion were intercrossed to generate mice homozygous for the allele. DNA from these pups was used to further verify the loss of all *Ugt2* genes by examination of both DNA and RNA from these animals. A probe was generated by PCR from exon 1 of *Ugt2b38* that is expected to bind to multiple sites throughout the deleted segment, including the first exons of *Ugt2b5*, *Ugt2b37*, *Ugt2b36*, and *Ugt2b35* as well as the intergenic region between *Ugt2a3* and *Ugt2b38*. Analysis of DNA from pups generated by intercross of heterozygous parents showed that this probe failed to bind to DNA from the homozygous *ΔUgt2* offspring (Fig. 2A). As expected, probes corresponding to regions flanking the deletion bound to the DNA from these animals and identified the predicted, novel DNA fragments generated by the recombination event.

RNA was prepared from the nasal epithelium and liver of homozygous *ΔUgt2* animals and their WT littermates. As expected, high levels of *Ugt2a1/2* expression were observed in epithelium from WT animals, while expression was absent in samples collected from the null mice (Fig. 2B). Expression of members of the *Ugt2b* subfamily and *Ugt2a3* were examined in RNA prepared from the liver. Again, expression of these genes was easily detected in the WT animals, whereas no signal was observed in *ΔUgt2* animals (Fig. 2C). Taken together, these data support the DNA analysis indicating that the *ΔUgt2* mice lack all *Ugt2b* and *Ugt2a* genes.

Development and Reproductive Behavior of the *ΔUgt2* Mouse. Mice lacking the *Ugt2* genes were present in litters at expected Mendelian ratios. The growth and development of the mice were normal, and they could not be distinguished by observation from their WT littermates. The human UGT2B enzymes, including UGT2B4, UGT2B7, UGT2B15, and UGT2B17, have been shown to participate in the glucuronidation of endogenous steroids as well as xenobiotics (Hum et al., 1999). Alteration in steroid metabolism could dramatically alter the development of primary and secondary sex organs, and thus impair

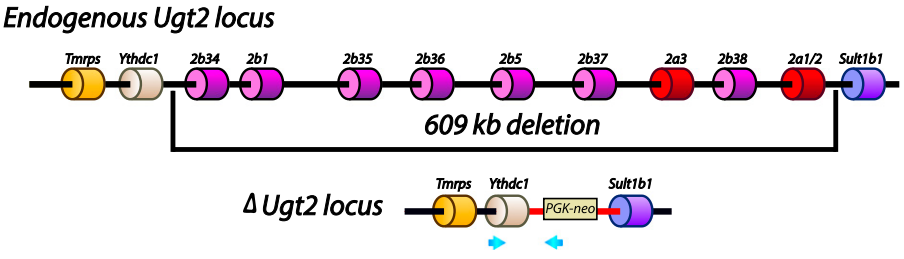

Fig. 1. Schematic drawing showing the structure of the WT and *ΔUgt2* loci. The locus includes all three *Ugt2a* and seven *Ugt2b* genes and is located between *Ythdc1* and *Sult1b1* on chromosome 5. The 609 kbp segment of DNA deleted during the homologous recombination event is indicated, and the structure of the *ΔUgt2* locus is shown below. The locus carries marker genes, and vector sequences are shown in red. The blue arrows show primers used in the initial screening of ES cell clones to identify those in which the deletion vector is inserted by homologous recombination.

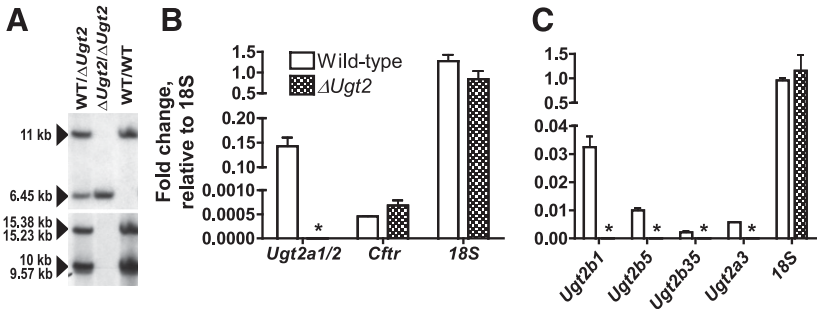

Fig. 2. Verification of the deletion of *Ugt2* genes. (A) DNA was prepared from tail biopsies of homozygous WT, homozygous *ΔUgt2*, and heterozygous pups, digested with *BamHI*, and analyzed by Southern blot. A probe corresponding to a region just outside the *Ugt2* locus was used to verify the genotypes of the mice and the integrity of the DNA. As predicted, it hybridized to 11 and 6.45 kbp DNA fragments corresponding to the WT allele and *ΔUgt2* locus, respectively (upper panel). The filter was then analyzed with a probe binding to *BamHI* fragments corresponding to a conserved region in *Ugt2a3*, *Ugt2b1*, *Ugt2b5*, and *Ugt2b35* (lower panel). The WT locus yielded four different fragments (15.38, 15.23, 10, and 9.57 kbp), as expected. Consistent with the excision of the entire Ugt2 locus during a single recombination event, no hybridization of the probe is observed in the lanes corresponding to the mice homozygous for the *ΔUgt2* locus. (B) RNA from olfactory epithelium was analyzed by quantitative PCR for *Ugt2a1/2*, normalized to 18S expression. As expected, robust expression is observed in WT mice, while none was detected in the *ΔUgt2* animals, as indicated by the asterisks. The quality and epithelial origin of the RNA was verified by showing that *Cftr* expression was robust and that the expression level did not differ between the *ΔUgt2* and WT animals. (C) RNA prepared from liver was analyzed by quantitative PCR for expression of *Ugt2b1*, *Ugt2b35*, *Ugt2b5*, and *Ugt2a3* and normalized to 18S expression. $N = 3$ for all samples and error bars represent the S.E.M.

the fecundity of mice. Therefore, we intercrossed mice homozygous for the *ΔUgt2* locus with WT littermates. The number of pups born to dams was within the normal size range (Supplemental Fig. 1). Furthermore, when *ΔUgt2* males were presented with fertile WT females, the interval until the first mating, the number of matings, the percentage of matings resulting in pregnancies, and the size of the resulting litters were not significantly different when compared with WT males (Supplemental Fig. 2). To further examine this point, male mice were sacrificed at 8 weeks, and their body weight and the sizes of their testes and seminiferous tubules were examined. No difference in the development of these organs was observed, consistent with the normal fertility of these animals (Supplemental Fig. 3). Serum testosterone levels measured in individually housed, 5 to 6 month old male mice did not differ significantly from controls (Supplemental Fig. 4).

Gene Expression. The health of the *ΔUgt2* animals could reflect compensation for the loss of *Ugt2* genes by increased expression of *Ugt1*s since substantial overlaps in the activities of these two enzyme families have been documented in both humans and rats (Radominska-Pandya et al., 1999; Lin and Wong, 2002; Bock, 2010). Increased expression of *Ugt1* isoforms in response to loss of the *Ugt2* genes would impact any conclusions drawn regarding observed differences in the metabolism of chemicals by the *ΔUgt2* animals. As mentioned previously, the *Ugt1* isoforms each have a unique 5′ exon. Primers specific for the first exons of *Ugt1a1*, *Ugt1a7*, and *Ugt1a9* were generated and each was paired with a common reverse primer corresponding to the shared second exon. Quantitative PCR analysis using these primers revealed that expression patterns for these three *Ugt1* mRNAs are similar to those reported previously (Buckley and Klaassen, 2007). When compared with WT mice, *ΔUgt2* mice showed no significant difference in expression of any of the three mRNAs in the adrenal gland, liver, prostate, epididymis, or testes (Fig. 3). This indicates that the normal development of these mice does not reflect compensation for loss of these genes by increased expression of UGT1 isoforms. These results also support the general usefulness of this mouse line for determining the contribution of the *Ugt2* genes to xenobiotic metabolism.

Naproxen Glucuronidation. To demonstrate the usefulness of the *ΔUgt2* mice in evaluation of the role of UGT2 enzymes in xenobiotic metabolism, we examined the ability of liver microsomes from these mice to metabolize naproxen. We chose this assay because a number of lines of evidence indicate that human and rat UGT2 isoforms show selectivity toward this substrate (el Mouelhi et al., 1987; Pritchard et al., 1994; Bowalgaha et al., 2005; Sanoh et al., 2012). Microsomes from *ΔUgt2* and co-isogenic WT controls were incubated with naproxen for 2 hours, and supernatant was analyzed by HPLC for the presence of the glucuronide. Microsomes from WT mice formed 46.2 ± 1.9 (mean ± S.E.M., $n = 3$) nmol of napG per mg microsomal protein, while microsomes from *ΔUgt2* mice showed no detectable amount of glucuronide formation (Fig. 4). These data indicate loss of activity against UGT2-specific substrates in the *ΔUgt2* animals and support the utility of this mouse line in assigning glucuronidation of xenobiotics to the *Ugt2* gene family.

BPA Glucuronidation. We next asked whether *ΔUgt2* mice could be used to measure the contribution of UGT2 enzymes to the metabolism of xenobiotics metabolized by both UGT families. Studies

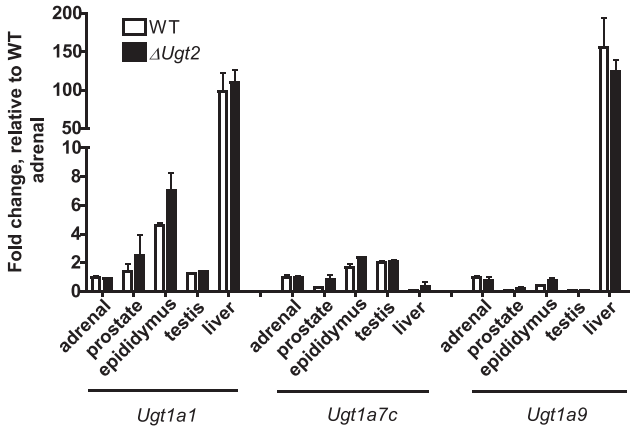

Fig. 3. Expression and tissue distribution of *Ugt1a* mRNAs in WT and *ΔUgt2* mice. *Ugt1a* expression levels were measured by quantitative real-time PCR with a SYBR Green quantitative PCR Master Mix. Primers were designed to amplify across the junction between the unique first exon for each isoform and the shared exons. cDNA samples were diluted to 10 pg/μl for amplification with the 18S probe and to 2.5 ng/μl for all other probes. The comparative threshold cycle method was used to quantify the relative gene expression. The amount of target was normalized to 18S as an endogenous reference and to WT adrenal gland as a calibrator. Expression of the examined isoforms did not differ significantly in any tissue examined between WT and *ΔUgt2* animals. Amplifications were performed in duplicate. Error bars represent the S.E.M. ($n = 3$).

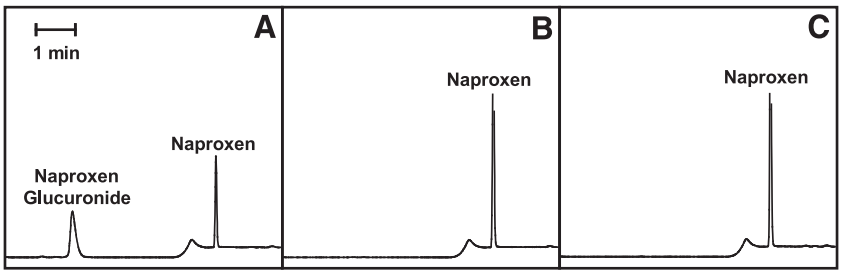

Fig. 4. Naproxen glucuronidation by liver microsomes from WT and *ΔUgt2* mice. Reactions contained 50–150 μg microsomal protein, 25 μg/ml alamethicin, 100 μM naproxen, and 5 mM UDPGA. (A) Typical chromatogram of reaction products of WT microsomes. (B) Typical chromatogram of reaction products of *ΔUgt2* microsomes. (C) Typical chromatogram of a control reaction lacking UDPGA. Microsomes from WT mice formed 46.2 ± 1.9 (mean ± S.E.M., $n = 3$) nmol NapG/mg of protein, while microsomes from *ΔUgt2* mice showed no detectable amount of glucuronide formation.

using recombinant human and rat UGTs have shown that BPA is a substrate for both enzyme families, with greater activity assigned to UGT2 enzymes (Yokota et al., 1999; Hanioka et al., 2008, 2011). Therefore, we first determined whether UGT2 enzymes are exclusively responsible for the metabolism of BPA by mouse microsomes. Microsomes prepared from pairs of WT and *ΔUgt* mice were incubated with BPA and the cofactor UDPGA for 2 hours. The quantities of BPA and BPAG in the reaction products were determined by HPLC. Under these conditions, rapid and complete metabolism of BPA was observed in reactions carried out using both WT and mutant microsomes. No difference was observed between *ΔUgt2* and WT microsomes in the total amount of BPAG produced (Fig. 5D). Thus, glucuronidation of BPA occurs in the absence of all UGT2 enzymes. Presumably, this conjugation is carried out by UGT1 enzymes. However, because the reactions were allowed to go to completion these experiments could not differentiate between the contributions of UGT1s and UGT2s to BPA glucuronidation.

By examining the kinetics of BPA glucuronidation in WT and *ΔUgt2* microsomes, the activities of the two enzyme families can be examined. The activity of WT microsomes is expected to represent the sum of the activities of the UGT1 and UGT2 families, whereas the activity of *ΔUgt2* microsomes represents that of the UGT1 family alone. Reaction conditions were optimized to allow measurement of differences in activity between WT and *ΔUgt2* microsomes by increasing the substrate-to-enzyme ratio and by removal of alamethicin. Alamethicin increases the rate of glucuronidation in microsomes by facilitating the movement of the substrate and UDPGA through the microsomal lipid bilayer. Thus, removal of alamethicin from the glucuronidation reactions decreased the reaction rates and facilitated kinetic analysis of the rapidly metabolized substrate. As shown in Fig. 5, under these conditions, the ability of UGT2 enzymes to contribute to BPA metabolism is easily observed. BPA glucuronidation exhibited Michaelis-Menten kinetics in both WT and *ΔUgt2* microsomes. Curves were fit to plots of glucuronidation rate (pmol/min/mg microsomal protein) versus BPA concentration (Fig. 5E). The kinetic parameters are given in Table 2. The V_{max} measured for *ΔUgt2* microsomes, which contain only UGT1 enzymes, is approximately 50% lower than that of WT microsomes, which contain UGT1s and UGT2s. This 50% decrease is attributed to the absence of the UGT2 enzymes in *ΔUgt2* microsomes. Thus, we concluded that 50% of the activity in WT microsomes was due to UGT2s and 50% to UGT1s, suggesting the activities of the two families are approximately equal. The K_m value did not differ significantly between the WT and the *ΔUgt2* microsomes. This suggests that, under these conditions, the two murine UGT families have approximately equal activity toward, and affinity for, BPA. To ensure that the exclusion of alamethicin did not alter the relative activities of microsomes derived from the two mouse lines, WT and *ΔUgt2* microsomes were incubated with 100 μM BPA either in the presence or absence of alamethicin. Significant differences between WT and *ΔUgt2* microsomes are present under both alamethicin-activated and nonactivated conditions, and the ratio of WT activity to *ΔUgt2* activity is comparable in both cases (Supplemental Fig. 5). This result is consistent with previous studies (Fisher et al., 2000) suggesting that alamethicin has an isoform-independent activating effect on UGTs.

To further evaluate the relative contributions of the two UGT families to microsomal BPA glucuronidation, we used our data sets to derive theoretical kinetic parameters for the UGT1 and UGT2 enzymes, assuming that all BPAG detected was formed by these two enzyme families. Since *ΔUgt2* mice express only UGT1 enzymes, the kinetic parameters of the *ΔUgt2* microsomes are assigned to the UGT1 family.

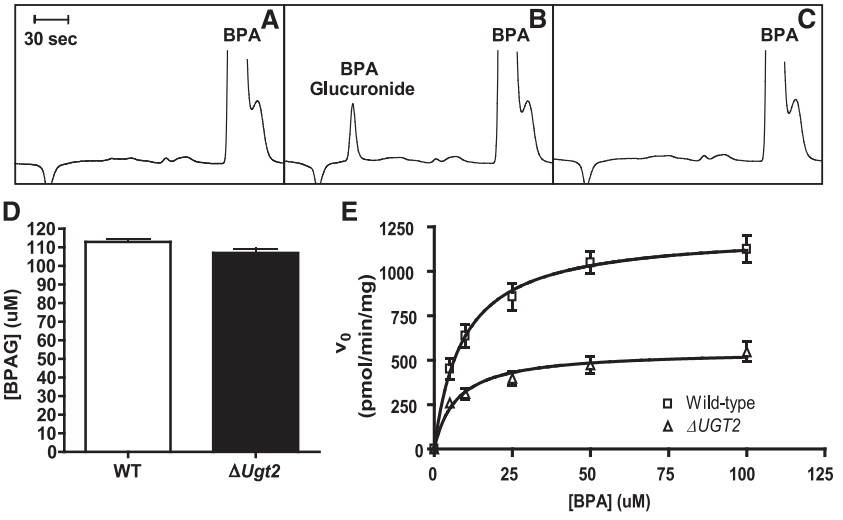

Fig. 5. BPA glucuronidation by liver microsomes from WT and *ΔUgt2* mice. (A) Typical chromatogram of products of a reaction terminated immediately after addition of UDPGA. (B) Typical chromatogram of products of a reaction terminated after 10 minutes of incubation. (C) The identity of the BPAG peak was verified by its loss after treatment with β-glucuronidase. (D) BPAG formation after 2-hour incubation of BPA and 25 μg/ml alamethicin with WT and *ΔUgt2* microsomes. Complete substrate conversion was observed, and BPAG concentrations were not significantly different. (E) Michaelis-Menten curves for glucuronidation of BPA by microsomes prepared from WT (squares) and *ΔUgt2* (triangles) mice in the absence of alamethicin. Each data point represents microsomal preparations from four mice. Error bars represent S.D. $r^2 > 0.95$ for WT mice and $r^2 > 0.85$ for *ΔUgt2* mice. Reactions contained 20–60 μg microsomal protein, 5–100 μM BPA, and 5 mM UDPGA.

TABLE 2

Kinetic parameters for BPA glucuronidation in liver microsomes from WT and *ΔUgt2* mice

Values are expressed as the mean ± S.D. (n = 4). V_{max} is significantly different at the $P < 0.0001$ level and K_m is not significantly different in unpaired Student's t tests.

	V_{max}	K_m
	pmol/min/mg	*μM*
WT	1220.0 ± 61.4	9.17 ± 1.73
ΔUgt2	553.2 ± 35.2	7.16 ± 1.87

Glucuronidation of BPA in WT microsomes was assumed to represent the sum of the activities of both UGT2 and UGT1 enzymes, and theoretical K_m and V_{max} values for the UGT2 family were derived using the two-enzyme Michaelis-Menten equation (Segel, 1993):

$$V_{WT} = \frac{(V_{max_{UGT1}})[S]}{K_{m_{UGT1}} + [S]} + \frac{(V_{max_{UGT2}})[S]}{K_{m_{UGT2}} + [S]}$$

where V is the rate of reaction; [S] is the concentration of the substrate; and K_m and V_{max} are the Michaelis constant for and maximum rate attributed to each UGT family, respectively. As shown subsequently, UGT2 activity can be represented by the difference in the glucuronidation rate between WT mice and *ΔUgt2* counterparts:

$$\frac{(V_{max_{UGT2}})[S]}{K_{m_{UGT2}} + [S]} = V_{WT} - \frac{(V_{max_{UGT1}})[S]}{K_{m_{UGT1}} + [S]} = V_{WT} - V_{\Delta Ugt2}$$

Thus, UGT2-mediated BPA glucuronidation was modeled using a Michaelis-Menten curve fitted to a plot of the difference in rate between paired WT and *ΔUgt2* microsomes at each substrate concentration (Fig. 6). The kinetic parameters are given in Table 3. Based on this analysis, the activities and affinities of the UGT1 and UGT2 enzymes toward BPA are predicted to be very similar.

BPA Metabolism In Vivo. Evaluation of BPA glucuronidation by *ΔUgt2* and WT microsomes indicates that UGT1 and UGT2 enzymes contribute equally to BPA metabolism. To determine whether this predicts the activities of these gene families in vivo, we examined the metabolism of BPA in WT and mutant animals. The bile ducts of paired WT and *ΔUgt2* male mice matched for weight and age were cannulated. After collection of a predose bile sample for use as a baseline control, each animal received a single bolus of BPA delivered intravenously. Fractions of bile were collected over the next 50 minutes, and the quantity of BPAG in each bile fraction was determined by HLPC. No significant difference was seen in the volume or rate of bile production by the *ΔUgt2* and WT animals, and BPAG accumulation in the bile was linear over the 50 minute collection in both mouse lines. The biliary excretion rate was therefore expressed as the fraction of the initial BPA dose excreted per minute.

As expected, based on the study of *ΔUgt2* microsomes, BPAG was detected in the bile of the *ΔUgt2* mice, clearly indicating that the UGT1 family glucuronidates BPA in vivo. More surprisingly, following a dose of 2 mg BPA/kg b.wt., no significant difference between the rate of biliary BPA excretion in WT and *ΔUgt2* mice was observed (Fig. 7). This result suggests that the impact of the UGT2 family on BPA clearance is minimal at this exposure level and that the UGT1 family has significant capacity for BPA conjugation in vivo. When the BPA dose was increased to 20 mg/kg b.wt., a significant decrease between the average biliary excretion rates for WT and *ΔUgt2* mice was observed. Approximately 0.31% of the BPA dose was glucuronidated and excreted per minute by WT mice. However, in mutants only 0.22% of the initial dose was glucuronidated and excreted per minute,

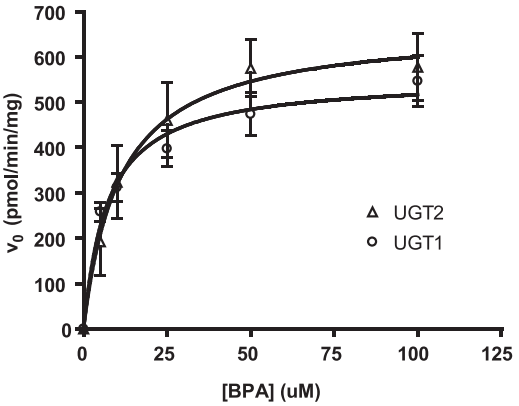

Fig. 6. Enzyme kinetics of UGT1- and UGT2-mediated BPA glucuronidation. The glucuronidation activity remaining in mutant mice after deletion of the *Ugt2*s was assigned to the UGT1 family (circles). The difference in glucuronidation rate measured between microsomes from WT and *ΔUgt2* animals was used to represent activity of the UGT2 family (triangles). The calculated kinetics of glucuronidation of BPA by both enzyme families was consistent with the Michaelis-Menten models. Calculations assumed equal concentrations of UGT1 and UGT2 enzymes in WT microsomes. $r^2 > 0.85$ for UGT1s and $r^2 > 0.75$ for UGT2s. Error bars represent the S.E.M., $n = 4$ microsomal preparations of each genotype.

approximately a 28% reduction in excretion rate (Fig. 7). A significant contribution of the UGT2s to BPA clearance was only observable at this extremely high dose of BPA. Male mice were used in these studies to avoid potential increases in animal-to-animal variation due to the estrous cycle in females; however, examination of hepatic BPA glucuronidation after a dosage of 2 mg BPA/kg b.wt. in female mice also failed to reveal a significant difference between WT and *ΔUgt2* animals (Supplemental Fig. 6). Thus, we conclude that the UGT1 family is primarily responsible for the rapid glucuronidation and clearance of BPA in male and female mice.

Discussion

In this study, we show the generation of mice lacking the ~600 kbp DNA segment carrying the *Ugt2* gene family. Unlike mice lacking the UGT1 enzymes (Nguyen et al., 2008), the mice are healthy and indistinguishable from control animals when bred in a specific pathogen–free animal facility. While the UGT1 family is essential for the conjugation and excretion of endogenous metabolites, our data indicate that the members of the UGT2 family do not play an essential and unique role in this function. Particularly surprising is the fact that the loss of UGT2 enzymes does not significantly alter sexual development or fertility, given the ability of both rodent and human UGT2s to metabolize steroid hormones, particularly androgens (Hum et al., 1999; Chouinard et al., 2008). Studies using mice lacking the androgen receptor or mice treated with antiandrogens such as cyproterone acetate have shown that the development of the secondary sex organs is sensitive to androgen levels (Jean-Faucher et al., 1984; Yeh et al., 2002). Both of these studies reported impaired development of secondary sex organs observable at a gross anatomic level as well as infertility when androgen metabolism was impaired. This indicates that the normal development of these organs is a sensitive surrogate marker for normal androgen metabolism in mice. A possible explanation for the lack of a developmental or reproductive phenotype in the mutants is that glucuronidation is not a critical pathway for androgen excretion in mice. There is evidence that sulfonation is the predominant excretory pathway for some substrates in rodents (Sanoh et al., 2012), and a number of steroid-conjugating sulfotransferases, including the estrogen-preferring SULT1E1 and the hydroxysteroid sulfotransferases

TABLE 3

Kinetic parameters for BPA glucuronidation by mouse UGT1s and UGT2s

Values are expressed as the mean ± S.E.M. (n = 4). Neither V_{max} nor K_m is significantly different in an unpaired Student's t test.

	V_{max}	K_m
	pmol/min/mg	*μM*
UGT2	665.5 ± 73.1	10.99 ± 4.27
UGT1	553.2 ± 35.2	7.16 ± 1.87

SULT2A1 and SULT2B1, could contribute to androgen metabolism (Alnouti and Klaassen, 2006). Supporting this possibility, neither the Gunn rat (Nguyen et al., 2008) nor the *ΔUgt2* mouse exhibits altered fertility or sexual development, while the *Sult1e1* knockout mouse exhibits alterations in both capacities (Qian et al., 2001).

The *Ugt2a* genes are located in the same cluster as the *Ugt2b* genes in both humans and rodents. *Ugt2a1* and *Ugt2a2* are expressed in the nasal epithelium, and studies using recombinant enzymes have shown that they are able to conjugate odorants. This is hypothesized to be important in the termination of odorant signaling and preventing receptor desensitization (Lazard et al., 1991; Sneitz et al., 2009). The *ΔUgt2* mouse line should allow this hypothesis to be tested, both in vitro using cultured nasal epithelial cells and in vivo using odor-dependent behavioral paradigms (Friedrich, 2006). While the function of *Ugt2a3* remains unclear (Buckley and Klaassen, 2009; Sneitz et al., 2009), its conservation across species suggests a role in excretion of endogenous metabolites (Mackenzie et al., 2005). However, our studies indicate that, at least in mice bred in a vivarium, this gene is not essential for normal development and health.

Previous studies using recombinant UGT2 enzymes indicate that the UGT2 family is important in the metabolism of many nonsteroidal anti-inflammatory drugs in both humans and rats (King et al., 2000). Using microsomes prepared from the *ΔUgt2* mice, we show that glucuronidation of naproxen is dependent on the UGT2 enzymes. Even after extended incubation, only the parent compound was detected in *ΔUgt2* microsomal reaction products. However, we cannot exclude the possibility that some glucuronidation may be detected at higher substrate concentrations due to low-affinity interaction with UGT1 isoforms. Such interactions have been observed using recombinant human UGT1s (Bowalgaha et al., 2005). Studies using recombinant rat UGT enzymes indicate that UGT2B1 shows high activity toward many nonsteroidal anti-inflammatory drugs, including naproxen (Ritter, 2000). While our studies only allow assignment to the UGT2 enzyme family and not individual isoforms, it is likely that naproxen metabolism in the mouse is dependent on *Ugt2b1* expression.

Extensive studies have confirmed widespread human exposure to BPA (Vandenberg et al., 2007), and studies carried out in both rats and mice indicate possible adverse effects of BPA on development and health (Kabuto et al., 2004; Richter et al., 2007; Vandenberg et al., 2007; Hanioka et al., 2008). Considerable resources have been directed toward determination of the health risks associated with BPA exposure. Despite the interest in this xenobiotic, the understanding of its metabolism is incomplete. BPA is rapidly glucuronidated in both humans and rodents and excreted through urine and bile, respectively. However, less is known regarding the enzymes primarily responsible for formation of the glucuronide. Assigning this activity to the individual enzymes of the UGT1 and UGT2 families has relied largely on studies using recombinant enzymes. Studies of both human and rat enzymes indicate that the UGT2s, specifically UGT2B15 in human and UGT2B1 in rat, show the highest activity toward BPA. Therefore, it has been assumed that the UGT2 family is critical for rapid clearance of this xenobiotic. Our results are not consistent with this model and indicate that UGT1 enzymes generate a larger proportion of BPAG in vivo. One possibility is that Ugt1a9, orthologous to the BPA-conjugating human UGT1A9 (Hanioka et al., 2008), is a pseudogene in rats but functional in mice (Mackenzie et al., 2005). Thus, the UGT1s may make a larger relative contribution to BPA glucuronidation in mice than in rats.

The role of the UGT1s in BPA metabolism became apparent upon incubation of BPA with microsomes isolated from *ΔUgt2* mice. When allowed to go to completion, reactions containing WT and *ΔUgt2* microsomes with equal initial concentrations of BPA formed equal concentrations of BPAG. A contribution of UGT2s to BPA metabolism could be defined by examining the rate of formation of the glucuronide, and a 50% reduction was observed in the V_{max} of *ΔUgt2* microsomes when compared with WT controls. The approximately equal contributions of UGT1s and UGT2s to BPA metabolism in these in vitro studies did not accurately predict the impact of UGT2 deficiency on BPA

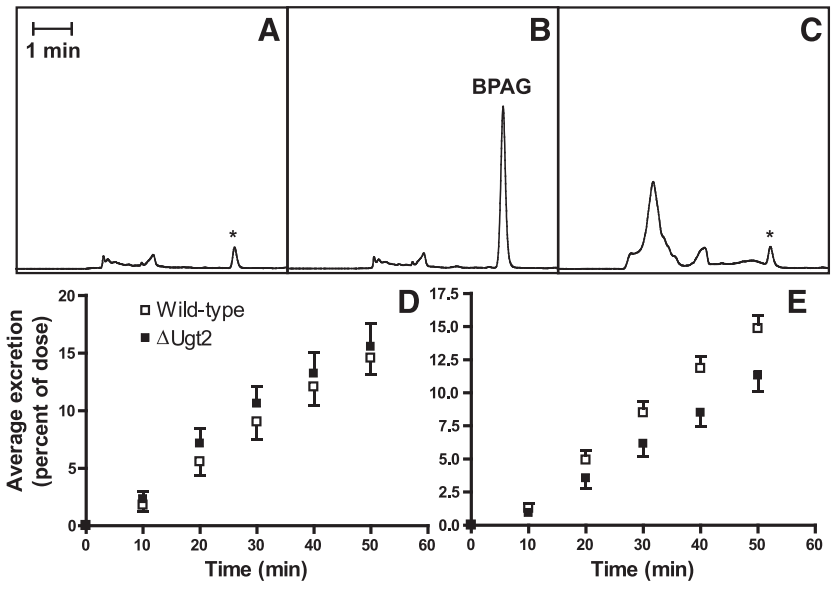

Fig. 7. In vivo BPA glucuronidation in WT and *ΔUgt2* mice. (A) Typical chromatogram of bile collected from a *ΔUgt2* mouse prior to dosage. (B) Typical chromatogram of a bile fraction collected from a *ΔUgt2* mouse from 0 to 10 minutes after dosage. (C) Treatment with β-glucuronidase causes loss of the BPAG peak and changes in the chromatographic profile due to deconjugation of endogenous glucuronides. BPAG peak areas were corrected for the area of a small interfering peak (presumably due to a co-eluting endogenous metabolite; marked by an asterisk) in bile obtained immediately before dosage. The interfering peak remained after β-glucuronidase treatment, indicating that it does not represent BPA exposure prior to experimentation. (D) Average BPAG excretion after dosage with 2 mg/kg BPA over the collection period for WT and *ΔUgt2* male mice, measured as percentage of dose/minute. Average excretion rates for WT and *ΔUgt2* mice were 0.306 ± 0.030 (mean ± S.E.M., $n = 3$) and 0.325 ± 0.039 (mean ± S.E.M., $n = 3$) respectively. (E) Average BPAG excretion after dosage with 20 mg/kg BPA over the collection period for WT and *ΔUgt2* mice. Average excretion rates for WT and *ΔUgt2* mice were 0.313 ± 0.019 (mean ± S.E.M., $n = 6$) and 0.224 ± 0.024 (mean ± S.E.M., $n = 7$) respectively. Average percent excretion/minute was significantly different at the $P < 0.05$ level in an unpaired Student's t test. BPAG excretion was linear over the time range examined (plots of percent excretion versus time had $r^2 > 0.93$ for all animals).

metabolism in vivo. At a dose of 2 mg/kg, orders of magnitude greater than the estimated 1.5 μg/kg exposure for the general human population (European Union, 2010), there was no significant difference in biliary BPA excretion between WT and $\Delta Ugt2$ mice. Only when the dosage was increased to 20 mg/kg was a significant difference observed. These data indicate that the UGT1 family has extensive capacity to glucuronidate BPA and that this enzyme family may, in fact, be primarily responsible for BPA metabolism in vivo. Barring extreme exposures, the contribution of UGT2s to hepatic conjugation of BPA may be negligible.

This work highlights the limitations of directly extrapolating the results of in vitro studies to in vivo metabolism of xenobiotics, which have been extensively discussed previously (Lin and Wong, 2002; Soars et al., 2002; Miners et al., 2006). In general, in vitro studies are reported to underestimate in vivo enzymatic activities. In the case of the $\Delta Ugt2$ mice, the in vitro results underestimated the contribution of the UGT1 family to BPA metabolism. One possible explanation could be the differential stability of mouse UGT2s and UGT1s during microsomal preparation or incubation, as has been observed in the glucuronidation of flavonoids (Joseph et al., 2007), thereby exaggerating the contribution of one family over the other in in vitro studies. It is also possible that differential localization of UGT1 and UGT2 enzymes in the liver results in differential access to BPA in an in vivo environment. Additional experiments, including evaluation of BPA metabolism by primary mouse hepatocytes, could help to distinguish between these possibilities.

Several human UGT isoforms are capable of conjugating BPA. UGT2B15 is reported to have the highest activity, with lower activities observed for recombinant UGT1A1, UGT1A3, UGT1A9, UGT2B4, and UGT2B7 (Hanioka et al., 2008). An important issue impacted by the assignment of BPA primarily to the UGT2 family is the ability of neonates to metabolize BPA. Neonates and infants have reduced levels of *UGT2* expression until 6 to 7 months of age. Therefore, they may represent a subpopulation with increased susceptibility to BPA's adverse effects (Strassburg et al., 2002; Zaya et al., 2006; Divakaran et al., 2014). Concern regarding the ability of the newborn to metabolize BPA is the basis for restricting the use of BPA-containing plastics in infant bottles in some countries. However, if human UGT1 enzymes contribute extensively to BPA metabolism, as we have found to be the case in mice, this concern may not be well-founded. UGT1A9 reaches adult levels by 4 months, and expression of UGT1A1 increases rapidly after birth due to the necessity of bilirubin conjugation, which occurs in the maternal liver via transfer across the placenta prior to birth (Schenker et al., 1964; Onishi et al., 1979; Miyagi et al., 2012). While we cannot rule out the possibility that the predominant role of UGT1s in BPA metabolism is unique to the mouse, the UGT1 family is more closely conserved between species than the UGT2 family, suggesting that members of the UGT1 family may play a major role in BPA glucuronidation in humans.

In summary, we describe here the generation of a mouse line allowing definitive assignment of metabolism of xenobiotics to the UGT1 or UGT2 enzyme family. The normal development and good health of these animals makes them an ideal model for such studies. Reconstitution of the deleted locus with individual mouse or human *UGT2* genes will provide a means of refining functional assignments to individual UGT2 enzymes in vivo.

Acknowledgments

The authors thank Dr. Brian Hogan for useful insights regarding enzyme kinetics, Dr. Linda Spremulli and Dr. Matthew Redinbo for helpful discussions, Anne Latour for ES cell work, Joseph Snouwaert for artwork, and Peter Repenning and Leonard Collins for expert technical assistance and advice.

Authorship Contributions

Participated in research design: Fay, Nguyen, Snouwaert, Grant, Bodnar, Koller.

Conducted experiments: Fay, Nguyen, Snouwaert, Dye, Koller.

Contributed new reagents or analytic tools: Bodnar.

Performed data analysis: Fay, Nguyen, Snouwaert, Dye, Koller.

Wrote or contributed to the writing of the manuscript: Fay, Snouwaert, Grant, Koller.

References

Alnouti Y and Klaassen CD (2006) Tissue distribution and ontogeny of sulfotransferase enzymes in mice. *Toxicol Sci* **93**:242–255.

Bock KW (2010) Functions and transcriptional regulation of adult human hepatic UDP-glucuronosyl-transferases (UGTs): mechanisms responsible for interindividual variation of UGT levels. *Biochem Pharmacol* **80**:771–777.

Bowalgaha K, Elliot DJ, Mackenzie PI, Knights KM, Swedmark S, and Miners JO (2005) S-Naproxen and desmethylnaproxen glucuronidation by human liver microsomes and recombinant human UDP-glucuronosyltransferases (UGT): role of UGT2B7 in the elimination of naproxen. *Br J Clin Pharmacol* **60**:423–433.

Buckley DB and Klaassen CD (2007) Tissue- and gender-specific mRNA expression of UDP-glucuronosyltransferases (UGTs) in mice. *Drug Metab Dispos* **35**:121–127.

Buckley DB and Klaassen CD (2009) Induction of mouse UDP-glucuronosyltransferase mRNA expression in liver and intestine by activators of aryl-hydrocarbon receptor, constitutive androstane receptor, pregnane X receptor, peroxisome proliferator-activated receptor α, and nuclear factor erythroid 2-related factor 2. *Drug Metab Dispos* **37**:847–856.

Chouinard S, Barbier O, and Bélanger A (2007) UDP-glucuronosyltransferase 2B15 (UGT2B15) and UGT2B17 enzymes are major determinants of the androgen response in prostate cancer LNCaP cells. *J Biol Chem* **282**:33466–33474.

Chouinard S, Yueh MF, Tukey RH, Giton F, Fiet J, Pelletier G, Barbier O, and Bélanger A (2008) Inactivation by UDP-glucuronosyltransferase enzymes: the end of androgen signaling. *J Steroid Biochem Mol Biol* **109**:247–253.

Coughtrie MW, Burchell B, Leakey JE, and Hume R (1988) The inadequacy of perinatal glucuronidation: immunoblot analysis of the developmental expression of individual UDP-glucuronosyltransferase isoenzymes in rat and human liver microsomes. *Mol Pharmacol* **34**: 729–735.

de Wildt SN, Kearns GL, Leeder JS, and van den Anker JN (1999) Glucuronidation in humans. Pharmacogenetic and developmental aspects. *Clin Pharmacokinet* **36**:439–452.

Divakaran K, Hines RN, and McCarver DG (2014) Human hepatic UGT2B15 developmental expression. *Toxicol Sci* **141**:292–299.

el Mouelhi M, Ruelius HW, Fenselau C, and Dulik DM (1987) Species-dependent enantioselective glucuronidation of three 2-arylpropionic acids. Naproxen, ibuprofen, and benoxaprofen. *Drug Metab Dispos* **15**:767–772.

European Union (2010) European Union Risk Assessment Report: 4,4′-Isopropylidenediphenol (bisphenol-A)—Part 2 human health, Human Health Addendum of April 2008, Publications Office of the European Union, Luxembourg.

Fang JL, Beland FA, Doerge DR, Wiener D, Guillemette C, Marques MM, and Lazarus P (2002) Characterization of benzo(*a*)pyrene-*trans*-7,8-dihydrodiol glucuronidation by human tissue microsomes and overexpressed UDP-glucuronosyltransferase enzymes. *Cancer Res* **62**: 1978–1986.

Fisher MB, Campanale K, Ackermann BL, VandenBranden M, and Wrighton SA (2000) In vitro glucuronidation using human liver microsomes and the pore-forming peptide alamethicin. *Drug Metab Dispos* **28**:560–566.

Friedrich RW (2006) Mechanisms of odor discrimination: neurophysiological and behavioral approaches. *Trends Neurosci* **29**:40–47.

Ginsberg G and Rice DC (2009) Does rapid metabolism ensure negligible risk from bisphenol A? *Environ Health Perspect* **117**:1639–1643.

Hanioka N, Naito T, and Narimatsu S (2008) Human UDP-glucuronosyltransferase isoforms involved in bisphenol A glucuronidation. *Chemosphere* **74**:33–36.

Hanioka N, Oka H, Nagaoka K, Ikushiro S, and Narimatsu S (2011) Effect of UDP-glucuronosyltransferase 2B15 polymorphism on bisphenol A glucuronidation. *Arch Toxicol* **85**: 1373–1381.

Hum DW, Bélanger A, Lévesque E, Barbier O, Beaulieu M, Albert C, Vallée M, Guillemette C, Tchernof A, and Turgeon D, et al. (1999) Characterization of UDP-glucuronosyltransferases active on steroid hormones. *J Steroid Biochem Mol Biol* **69**:413–423.

Jean-Faucher C, Berger M, De Turckheim M, Veyssiere G, and Jean C (1984) Sexual maturation in male mice treated with cyproterone acetate from birth to puberty. *J Endocrinol* **102**:103–107.

Jedlitschky G, Cassidy AJ, Sales M, Pratt N, and Burchell B (1999) Cloning and characterization of a novel human olfactory UDP-glucuronosyltransferase. *Biochem J* **340**:837–843.

Joseph TB, Wang SWJ, Liu X, Kulkarni KH, Wang J, Xu H, and Hu M (2007) Disposition of flavonoids via enteric recycling: enzyme stability affects characterization of prunetin glucuronidation across species, organs, and UGT isoforms. *Mol Pharm* **4**:883–894.

Kabuto H, Amakawa M, and Shishibori T (2004) Exposure to bisphenol A during embryonic/fetal life and infancy increases oxidative injury and causes underdevelopment of the brain and testis in mice. *Life Sci* **74**:2931–2940.

Kaivosaari S (2010) N-Glucuronidation of drugs and other xenobiotics, Academic dissertation, University of Helsinki, Helsinki, Finland.

King CD, Rios GR, Green MD, and Tephly TR (2000) UDP-glucuronosyltransferases. *Curr Drug Metab* **1**:143–161.

Krishnan AV, Stathis P, Permuth SF, Tokes L, and Feldman D (1993) Bisphenol-A: an estrogenic substance is released from polycarbonate flasks during autoclaving. *Endocrinology* **132**: 2279–2286.

Kutsuno Y, Sumida K, Itoh T, Tukey RH, and Fujiwara R (2013) Glucuronidation of drugs in humanized UDP-glucuronosyltransferase 1 mice: Similarity with glucuronidation in human liver microsomes. *Pharmacol Res Perspect* **1**:e00002.

Lazard D, Zupko K, Poria Y, Nef P, Lazarovits J, Horn S, Khen M, and Lancet D (1991) Odorant signal termination by olfactory UDP glucuronosyl transferase. *Nature* **349**:790–793.

Lin JH and Wong BK (2002) Complexities of glucuronidation affecting in vitro in vivo extrapolation. *Curr Drug Metab* **3**:623–646.
Luconi M, Forti G, and Baldi E (2002) Genomic and nongenomic effects of estrogens: molecular mechanisms of action and clinical implications for male reproduction. *J Steroid Biochem Mol Biol* **80**:369–381.
Mackenzie PI, Bock KW, Burchell B, Guillemette C, Ikushiro S, Iyanagi T, Miners JO, Owens IS, and Nebert DW (2005) Nomenclature update for the mammalian UDP glycosyltransferase (UGT) gene superfamily. *Pharmacogenet Genomics* **15**:677–685.
Matthews JB, Twomey K, and Zacharewski TR (2001) In vitro and in vivo interactions of bisphenol A and its metabolite, bisphenol A glucuronide, with estrogen receptors α and β. *Chem Res Toxicol* **14**:149–157.
Miners JO, Knights KM, Houston JB, and Mackenzie PI (2006) In vitro–in vivo correlation for drugs and other compounds eliminated by glucuronidation in humans: pitfalls and promises. *Biochem Pharmacol* **71**:1531–1539.
Miyagi SJ, Milne AM, Coughtrie MW, and Collier AC (2012) Neonatal development of hepatic UGT1A9: implications of pediatric pharmacokinetics. *Drug Metab Dispos* **40**: 1321–1327.
National Research Council (2011) Guide for the Care and Use of Laboratory Animals, Eighth Edition, National Academies Press, Washington D.C.
Nguyen N, Bonzo JA, Chen S, Chouinard S, Kelner MJ, Hardiman G, Bélanger A, and Tukey RH (2008) Disruption of the *ugt1* locus in mice resembles human Crigler-Najjar type I disease. *J Biol Chem* **283**:7901–7911.
Onishi S, Kawade N, Itoh S, Isobe K, and Sugiyama S (1979) Postnatal development of uridine diphosphate glucuronyltransferase activity towards bilirubin and 2-aminophenol in human liver. *Biochem J* **184**:705–707.
Owens IS, Basu NK, and Banerjee R (2005) UDP-glucuronosyltransferases: gene structures of *UGT1* and *UGT2* families. *Methods Enzymol* **400**:1–22.
Pritchard M, Fournel-Gigleux S, Siest G, Mackenzie P, and Magdalou J (1994) A recombinant phenobarbital-inducible rat liver UDP-glucuronosyltransferase (UDP-glucuronosyltransferase 2B1) stably expressed in V79 cells catalyzes the glucuronidation of morphine, phenols, and carboxylic acids. *Mol Pharmacol* **45**:42–50.
Qian YM, Sun XJ, Tong MH, Li XP, Richa J, and Song WC (2001) Targeted disruption of the mouse estrogen sulfotransferase gene reveals a role of estrogen metabolism in intracrine and paracrine estrogen regulation. *Endocrinology* **142**:5342–5350.
Radominska-Pandya A, Czernik PJ, Little JM, Battaglia E, and Mackenzie PI (1999) Structural and functional studies of UDP-glucuronosyltransferases. *Drug Metab Rev* **31**:817–899.
Radominska-Pandya A, Little JM, and Czernik PJ (2001) Human UDP-glucuronosyltransferase 2B7. *Curr Drug Metab* **2**:283–298.
Richter CA, Birnbaum LS, Farabollini F, Newbold RR, Rubin BS, Talsness CE, Vandenbergh JG, Walser-Kuntz DR, and vom Saal FS (2007) In vivo effects of bisphenol A in laboratory rodent studies. *Reprod Toxicol* **24**:199–224.
Ritter JK (2000) Roles of glucuronidation and UDP-glucuronosyltransferases in xenobiotic bioactivation reactions. *Chem Biol Interact* **129**:171–193.
Rowland A, Miners JO, and Mackenzie PI (2013) The UDP-glucuronosyltransferases: their role in drug metabolism and detoxification. *Int J Biochem Cell Biol* **45**:1121–1132.
Sanoh S, Horiguchi A, Sugihara K, Kotake Y, Tayama Y, Uramaru N, Ohshita H, Tateno C, Horie T, and Kitamura S, et al. (2012) Predictability of metabolism of ibuprofen and naproxen using chimeric mice with human hepatocytes. *Drug Metab Dispos* **40**:2267–2272.
Schenker S, Dawber NH, and Schmid R (1964) Bilirubin metabolism in the fetus. *J Clin Invest* **43**:32–39.
Segel IH (1993) *Enzyme Kinetics: Behavior and Analysis of Rapid Equilibrium and Steady-State Enzyme Systems*, Wiley, New York.
Sneitz N, Court MH, Zhang X, Laajanen K, Yee KK, Dalton P, Ding X, and Finel M (2009) Human UDP-glucuronosyltransferase UGT2A2: cDNA construction, expression, and functional characterization in comparison with UGT2A1 and UGT2A3. *Pharmacogenet Genomics* **19**:923–934.
Soars MG, Burchell B, and Riley RJ (2002) In vitro analysis of human drug glucuronidation and prediction of in vivo metabolic clearance. *J Pharmacol Exp Ther* **301**:382–390.
Strassburg CP, Strassburg A, Kneip S, Barut A, Tukey RH, Rodeck B, and Manns MP (2002) Developmental aspects of human hepatic drug glucuronidation in young children and adults. *Gut* **50**:259–265.
Vandenberg LN, Hauser R, Marcus M, Olea N, and Welshons WV (2007) Human exposure to bisphenol A (BPA). *Reprod Toxicol* **24**:139–177.
Völkel W, Colnot T, Csanády GA, Filser JG, and Dekant W (2002) Metabolism and kinetics of bisphenol A in humans at low doses following oral administration. *Chem Res Toxicol* **15**: 1281–1287.
Yeh S, Tsai MY, Xu Q, Mu XM, Lardy H, Huang KE, Lin H, Yeh SD, Altuwaijri S, and Zhou X, et al. (2002) Generation and characterization of androgen receptor knockout (ARKO) mice: an in vivo model for the study of androgen functions in selective tissues. *Proc Natl Acad Sci USA* **99**:13498–13503.
Yokota H, Iwano H, Endo M, Kobayashi T, Inoue H, Ikushiro S, and Yuasa A (1999) Glucuronidation of the environmental oestrogen bisphenol A by an isoform of UDP-glucuronosyltransferase, UGT2B1, in the rat liver. *Biochem J* **340**:405–409.
Zaya MJ, Hines RN, and Stevens JC (2006) Epirubicin glucuronidation and UGT2B7 developmental expression. *Drug Metab Dispos* **34**:2097–2101.

Address correspondence to: Beverly H. Koller, 5073 Genetic Medicine Building, CB 7264, 120 Mason Farm Road, Chapel Hill, NC 27599. E-mail: treawouns@aol.com